

## RESEARCH ARTICLE

10.1029/2018JA025481

## Key Points:

- The impact of seven largest solar proton events on the mesospheric compositions during solar cycle 24 was discussed
- The variations of HO<sub>2</sub> and ozone were composed separately, and their general response to the solar proton events was analyzed
- The ozone depletion is found to be 1-day delay relative to the HO<sub>2</sub> increment during the solar proton events for the first time

## Correspondence to:

X. Xue,  
xuexh@ustc.edu.cn

## Citation:

Zou, Z., Xue, X., Shen, C., Yi, W., Wu, J., Chen, T., & Dou, X. (2018). Response of Mesospheric HO<sub>2</sub> and O<sub>3</sub> to Large Solar Proton Events. *Journal of Geophysical Research: Space Physics*, 123, 5738–5746. <https://doi.org/10.1029/2018JA025481>

Received 16 MAR 2018

Accepted 13 JUN 2018

Accepted article online 26 JUN 2018

Published online 7 JUL 2018

Response of Mesospheric HO<sub>2</sub> and O<sub>3</sub> to Large Solar Proton Events

Zicheng Zou<sup>1,2</sup> , Xianghui Xue<sup>1,2,3</sup> , Chenglong Shen<sup>1,3</sup> , Wen Yi<sup>1,2</sup> , Jianfei Wu<sup>1,2</sup> , Tingdi Chen<sup>1,2</sup> , and Xiankang Dou<sup>1</sup> 
<sup>1</sup>CAS Key Laboratory of Geospace Environment, Department of Geophysics and Planetary Sciences, University of Science and Technology of China, Hefei, China, <sup>2</sup>Mengcheng National Geophysical Observatory, School of Earth and Space Sciences, University of Science and Technology of China, Hefei, China, <sup>3</sup>Synergetic Innovation Center of Quantum Information and Quantum Physics, University of Science and Technology of China, Hefei, China

**Abstract** A lot of solar proton events (SPEs) have happened during the ongoing solar cycle 24 including extremely large events. Seven large SPEs from 2012 to 2017 were chosen to find the response of polar atmosphere to them. Three SPEs happened in 2012, and the other four SPEs happened in 2013, 2014, 2015, and 2017, respectively. The National Oceanic and Atmospheric Administration Geostationary Operational Environmental Satellites 13 proton observations were used to illustrate the proton flux toward the Earth during each SPE. These energetic protons are deposited in the middle and upper atmosphere and ionize the neutral atmosphere constituents and create radicals HO<sub>x</sub> (H, OH, and HO<sub>2</sub>). Enhancements in the upper atmospheric hydroperoxyl radical (HO<sub>2</sub>) of both polar regions of over 1 ppbv are found in the Aura Microwave Limb Sounder measurements immediately after some SPEs happened. The Microwave Limb Sounder observations of ozone (O<sub>3</sub>) show decreases of >10% in both polar middle and upper atmosphere for a few days with a peak value of >20–60% over 1–3 days. The compositions of HO<sub>2</sub> and ozone for all the selected SPEs indicate that the polar ozone depletions during the SPEs in a way are the result of the HO<sub>2</sub> enhancements.

## 1. Introduction

Coronal mass ejections can release large quantities of matter and electromagnetic radiation into interplanetary. The protons, which carry most of the energy of the fluxes, deposit along the Earth's magnetic field and impact the polar middle and upper atmosphere causing ionizations, dissociations, dissociative ionizations, and excitations (Frederick, 1976). This kind of period is known as solar proton event (SPE). Since 1940s, people have discovered the influence of SPE and have developed various methods to detect it (Heath et al., 1977; Newell & Naugle, 1960). During an SPE, the proton-induced interactions lead to the production of HO<sub>x</sub> (H, OH, and HO<sub>2</sub>), NO<sub>x</sub> (N, NO, and NO<sub>2</sub>), as well as other constituents such as N<sub>2</sub>O within polar cap region (Crutzen et al., 1975; Funke et al., 2008; Jackman et al., 2009; Seppälä et al., 2004). The hydrogen radical (OH and HO<sub>2</sub>) caused by SPE are short-lived, but both of them can induce ozone decreases persisting up to several days (e.g., Frederick, 1976; Jackman et al., 2005a, 2005b; Swider & Keneshea, 1973; von Clarmann et al., 2013).

The proton fluxes, which are more frequent and stronger during solar maximum, can intensely disturb the atmospheric composition. The influences of the SPEs on the middle and upper atmosphere have been greatly studied (e.g., Funke et al., 2008; Heath et al., 1977; Jackman et al., 2005a, 2005b, 2014; Krivolutsky et al., 2006; López-Puertas et al., 2005; Sinnhuber et al., 2012; Solomon et al., 1981; Swider & Keneshea, 1973; Verkhoglyadova et al., 2016; Verronen et al., 2011, 2006; von Clarmann et al., 2005). Due to different features, each new event can help us to comprehend the SPE-caused atmospheric disturbance deeper. Although several large SPEs have happened in recent years, most researchers are interested in the effect of specific SPEs on the atmospheric compositions or just focus on the SPEs themselves (Emslie et al., 2012; Gopalswamy et al., 2014; McPeters & Jackman, 1985; Shea & Smart, 2012; Verkhoglyadova et al., 2015, 2016). Few of them explored the general influence on the atmospheric compositions and of the SPEs during the solar cycle 24 and the correlation between variations of the neutral components after the SPEs.

The high reactivity makes the hydrogen radical of particular importance in atmospheric chemistry. During the SPEs, the increases in mesospheric OH have been observed (Damiani et al., 2010; Jackman et al., 2011;

**Table 1***List of Seven Large Solar Proton Events Selected Within Solar Cycle 24 With Start Date, Time (UT), and Maximum Proton Flux (Particle Flux Unit)*

No.	Date	Time (UT)	Peak proton flux (pfu > 10 MeV)
1	23 January 2012	0530	6,260
2	7 March 2012	0510	5,460
3	17 May 2012	0210	255
4	22 May 2013	1420	1,660
5	6 January 2014	0915	1,030
6	21 June 2015	2135	1,070
7	10 September 2017	1645	1,490

Verkhoglyadova et al., 2015, 2016; Verronen et al., 2006). Jackman et al. (2014) compared the observations and model predictions and showed a good simulation of hydrogen radical and ozone during large SPEs. The recent study of Verkhoglyadova et al. (2016) quantified the effects of combined solar protons and magnetospheric electrons fluxes on nighttime OH density enhancements during two SPEs, helping us to further understand the ionization-driven changes in mesospheric composition and potential short-time mesospheric ozone destruction.

In this paper, we use Geostationary Operational Environmental Satellites 13 (GOES 13) proton and Microwave Limb Sounder (MLS)

atmospheric composition measurements to study the general influence of the SPEs between 2012 and 2017 within the solar cycle 24. First, we show the proton flux toward the Earth during the SPEs. Then we calculate the variations of middle and upper atmospheric HO<sub>2</sub> and ozone compositions over polar regions separately. Finally, we compose the variations during different SPEs together showing a general response of ozone and HO<sub>2</sub> to SEP (solar energetic particles) and finding the relation between ozone and HO<sub>2</sub>.

## 2. SPE Selection and Proton Flux

National Oceanic and Atmospheric Administration (NOAA) Space Environment Services Center defines the start of a proton event to be the first of 3 integral 5-min average data points with fluxes greater than or equal to 10 pfu (particles/sr cm<sup>2</sup> s). The end of an event is the last time the flux was greater than or equal to 10 pfu. To find a significant influence on the middle and upper atmosphere due to the SPE, we select seven largest SPEs from 2012 to 2017. These SPEs are listed in Table 1. The fourth column of Table 1 is the maximum proton flux particles for energies larger than 10 MeV during each SPE. All of these maxima are greater than 1,000 except the third one during May 2012. This event was chosen in the list for the reason that it caused a ground level enhancement (GLE) event (Gopalswamy et al., 2013; Li et al., 2013). We can see that its higher energy proton flux is comparable to the other selected SPEs' proton.

The energetic particle data (proton energies from 1 to 300 MeV) are provided by the NOAA Space Weather Prediction Center for the NOAA GOES 13. The GOES 13 data sets have been used as the source of protons depositing energy into polar regions (Jackman et al., 2014). The proton fluxes during each SPEs are given in Figure 1 in five energy intervals (>1, >10, >30, >50, and >100 MeV). We can see that the flux increased by 2 to 3 orders of magnitude during these SPEs for most energy levels.

Jackman et al. (1980) discussed an energy deposition methodology to calculate the ion pair production rate using the proton flux data. The computed daily average data are a function of pressure between 888 hPa and  $8 \times 10^{-5}$  hPa and can be assumed to affect the atmosphere over the polar regions. The maximum computed ionization rates, pressure of the maximum value, and the pressure domain of mainly ionization pressure height for the events are listed in Table 2. The mainly ionization pressure domain is defined as the computed values larger than  $0.5 \times$  maximum computed value. During most events, the deposited protons can produce ion pairs significantly at pressure above 0.306 hPa.

## 3. Hydroperoxyl Radical (HO<sub>2</sub>)

At high latitudes, one of the major sources of the change in mesospheric HO<sub>x</sub> from positive ion chemistry is the ion pair produced by SEP. Solomon et al. (1981) have given the HO<sub>x</sub> production as a function of altitude and ion pair production rate. In the computation, an ion pair typically produces no more than two HO<sub>x</sub> constituents. This made it inevitable that HO<sub>2</sub> constituents will be impacted by ion pair production.

In contrast to energetic electron precipitation, which are first stored and energized in the radiation belts (Andersson et al., 2014; Brown, 1968; Verronen et al., 2011; Zawedde et al., 2016), solar protons propagate directly into the polar atmosphere as soon as they approach the Earth and lead to HO<sub>2</sub> vary rapidly

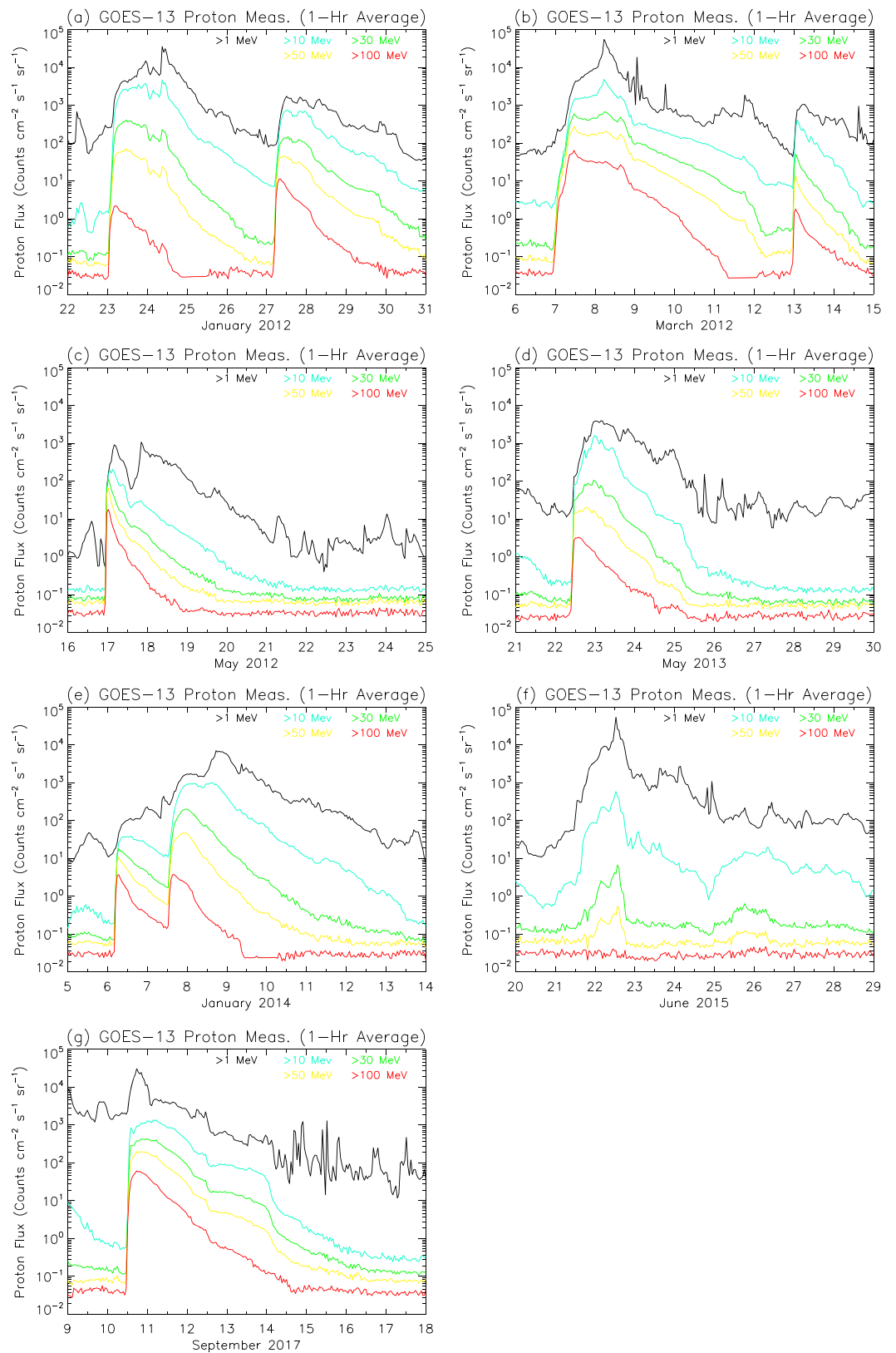


**Figure 1.** One-hour average Geostationary Operational Environmental Satellites 13 proton flux measurements in (a) January 2012, (b) March 2012, (c) May 2012, (d) May 2013, (e) January 2014, (f) June 2015, and (g) September 2017 for energies  $>1$  MeV (black),  $>10$  MeV (blue),  $>30$  MeV (green),  $>50$  MeV (light yellow), and  $>100$  MeV (red).

**Table 2***Maximum Computed Ionization Rates, Pressure of the Maximum Value, and the Pressure Domain of Mainly Ionization Pressure Height for the Events in Table 1*

Date of maximum value	Maximum computed values (ion pair/[cm <sup>3</sup> s])	Pressure of maximum value (hPa)	Pressure domain of mainly ionization <sup>a</sup> (hPa)
24 January 2012	2,858	0.042	0.306–0.006
8 March 2012	3,039	0.024	0.540–0.003
17 May 2012	74	0.406	5.255–0.010
23 May 2013	808	0.074	0.306–0.013
9 January 2014	779	0.031	0.130–0.003
22 June 2015	1,425	0.008	0.031–0.002
11 September 2017	1,217	0.024	1.685–0.002

<sup>a</sup>The mainly ionization domain is where the computed values larger than  $0.5 \times$  maximum value.

(approximately hours) through photochemical reactions (Nicolet, 1975; Solomon et al., 1983). Thus, a 5-day average before the SPE as a background is sufficient for the HO<sub>2</sub> level.

The MLS carried by the Aura satellite provides the HO<sub>2</sub> observations covering the time range of our research in the middle and upper atmosphere. Livesey et al. (2018) provide the methods and considerations for processing data. The highest latitude that MLS can reach is 82.5°N and 82.5°S. Thus, we choose 60–82.5°N and 60–82.5°S bands as the polar regions the same as that used in Jackman et al. (2014). Figure 2 shows the daily averaged flux of proton with energies >10 MeV from GOES 13, and the mixing ratio changes of HO<sub>2</sub> from the background HO<sub>2</sub>, which is obtained using a 5-day averaged HO<sub>2</sub> before SPE, in both polar regions for every event. For example, the first SPE in the list started at 23 January 2012; thus, the background is the average from 18 to 22 January and the figures show the HO<sub>2</sub> change from 20 to 28 January containing 3 days before SPE as a comparison. The left panel of Figure 2 is the HO<sub>2</sub> constituent change in the northern polar mesosphere, and the right panel is the HO<sub>2</sub> constituent change in the southern polar mesosphere.

All the SPEs resulted in greater than 0.2-ppbv enhancements of HO<sub>2</sub> from 0.1 to 0.046 hPa. Limited by MLS's HO<sub>2</sub> observation range, we believe that HO<sub>2</sub> will increase at a little higher altitude. One peak of larger than 1 ppbv is observed from ~0.046 to 0.1 hPa on 24 January in the northern hemisphere. Five peaks of >0.5 ppbv are also observed in other events or hemisphere. The peaks of proton fluxes and HO<sub>2</sub> increments mostly occurred the day after the SPE started, except the 6–9 January 2014 SPE. An unusually large peak covering the entire MLS HO<sub>2</sub> useful range appeared on 10 January 2014. Though there was a GLE in the fifth SPE (Thakur et al., 2014), the peak of HO<sub>2</sub> enhancement appears 2 days later than the peak of proton flux that occurred on 7 January. This HO<sub>2</sub> peak may be caused by other mechanisms caused by GLE that is different from the other SPEs listed in Table 1. In the same event, the difference of magnitude and duration of HO<sub>2</sub> enhancement between the northern and southern mesosphere partly depends on the season the SPE occurred. The first, the second, and the fifth SPEs have a large and a slightly long lasting HO<sub>2</sub> enhancement in northern mesosphere, which occurred in January, March, and January, respectively. The fourth and the seventh SPEs have a large and a slightly long lasting HO<sub>2</sub> enhancement in the southern mesosphere, which occurred in May and September. The HO<sub>2</sub> production is roughly the same in both hemispheres during the third and the sixth SPEs. But the lifetime of HO<sub>2</sub> is longer in the northern polar mesosphere during the third SPE and in the southern polar mesosphere during the sixth SPE. In general, the larger perturbation HO<sub>2</sub> variations are more likely to occur in winter. In summer, the intense solar radiation may increase the rate of photochemical reactions then diminish the duration of the disturbance.

The background also depends on the season. The HO<sub>2</sub> background concentration in the summer polar mesosphere (southern hemisphere in the first, the second, and the fifth SPEs and northern hemisphere in the third, the fourth, the sixth, and the seventh SPEs for the ~0.046–1.00 hPa region) is ~0.1–1 ppbv greater than that in the winter polar mesosphere (northern hemisphere in the first, the second, and the fifth SPEs and southern hemisphere in the third, the fourth, the sixth, and the seventh SPEs for the ~0.046–1.00 hPa region).

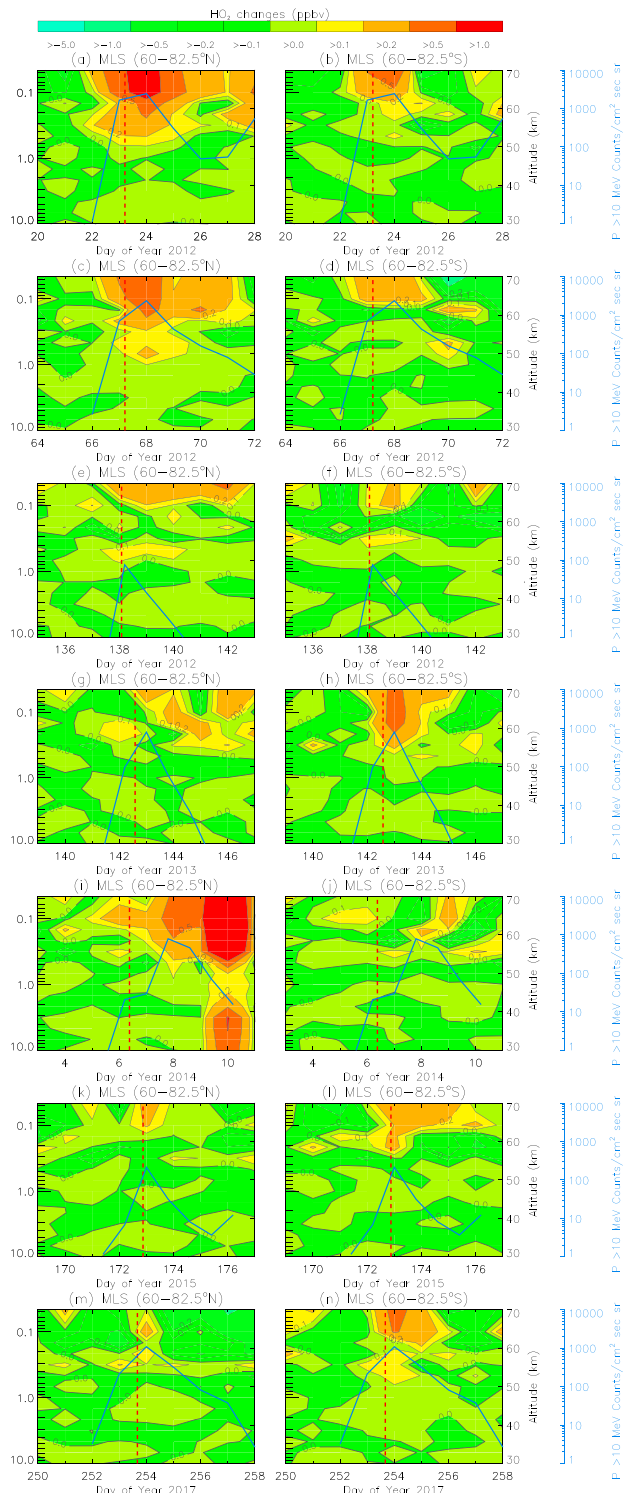


**Figure 2.** Daily averaged flux of proton with energies  $>10$  MeV from Geostationary Operational Environmental Satellites 13 and mixing ratio changes of  $\text{HO}_2$  from Aura Microwave Limb Sounder for the (left)  $60\text{--}82.5^\circ\text{N}$  band and (right)  $60\text{--}82.5^\circ\text{S}$  band. Each numbered row corresponds to the numbered solar proton event (SPE) listed in Table 1. The contour intervals for the  $\text{HO}_2$  changes are  $-1.0$ ,  $-0.5$ ,  $-0.2$ ,  $-0.1$ ,  $0.0$ ,  $0.1$ ,  $0.2$ ,  $0.5$ , and  $1.0$  ppbv. The blue lines are the daily averaged proton flux during the SPEs. The dotted red lines indicate the start time of the SPEs.

#### 4. Ozone ( $\text{O}_3$ )

It has been confirmed that ozone can be decomposed by the catalysis of  $\text{HO}_x$  constituents in the middle and upper atmosphere. Especially during SPEs, the brief increased  $\text{HO}_x$  in the mesosphere will cause ozone depletion (Swider & Keneshea, 1973) around the altitude of the disturbance. Solomon et al. (1983) have reported several catalytic processes destroying the mesospheric ozone, and Jackman et al. (2014) suggested that the following catalytic  $\text{HO}_x$  cycle



and



net:



plays a major role in decomposing the ozone in the quiet period all over the mesosphere.

And another process



and



net:



will also lead to the ozone decomposition during strong SPEs at the same altitude, due to the  $\text{HO}_2$  increase.

The daily averaged flux of proton with energies  $>10$  MeV and MLS observed polar mesospheric ozone variations during these strong SPEs in Table 1 are shown in Figure 3. Using the similar method, a 5-day averaged background is taken away. The left and right panels are the changes in the northern and southern polar regions, respectively. All SPEs resulted in significant ozone decrease within the range of  $0.02\text{--}1.0$  hPa. The ozone reduced more than 60% in the first and second SPEs in winter hemisphere, and both kept the magnitude for 3 days. A range of  $10\text{--}40\%$  depletion occurred during others SPEs. A short-time increase in  $\text{HO}_2$  can result in a substantial reduction in ozone over a longer period of time.

There appears to be a negative correlation between the variations of  $\text{HO}_2$  and ozone. An increase of  $\text{HO}_2$  more than  $0.5$  ppbv always leads to significant and longer-lasting ozone depletion. The  $\text{HO}_2$  increases in 24 January 2012 around  $0.1$  hPa in the Arctic region, and the Antarctic region both caused an ozone depletion for almost the same height range in 24 January 2012. A similar situation occurred around  $0.1$  hPa in 8 March 2012, 23 May 2014, and 11 September 2017 in the southern hemisphere. The increase of  $\text{HO}_2$  and the decrease of ozone have a high morphology similarity in space and time. Most of the



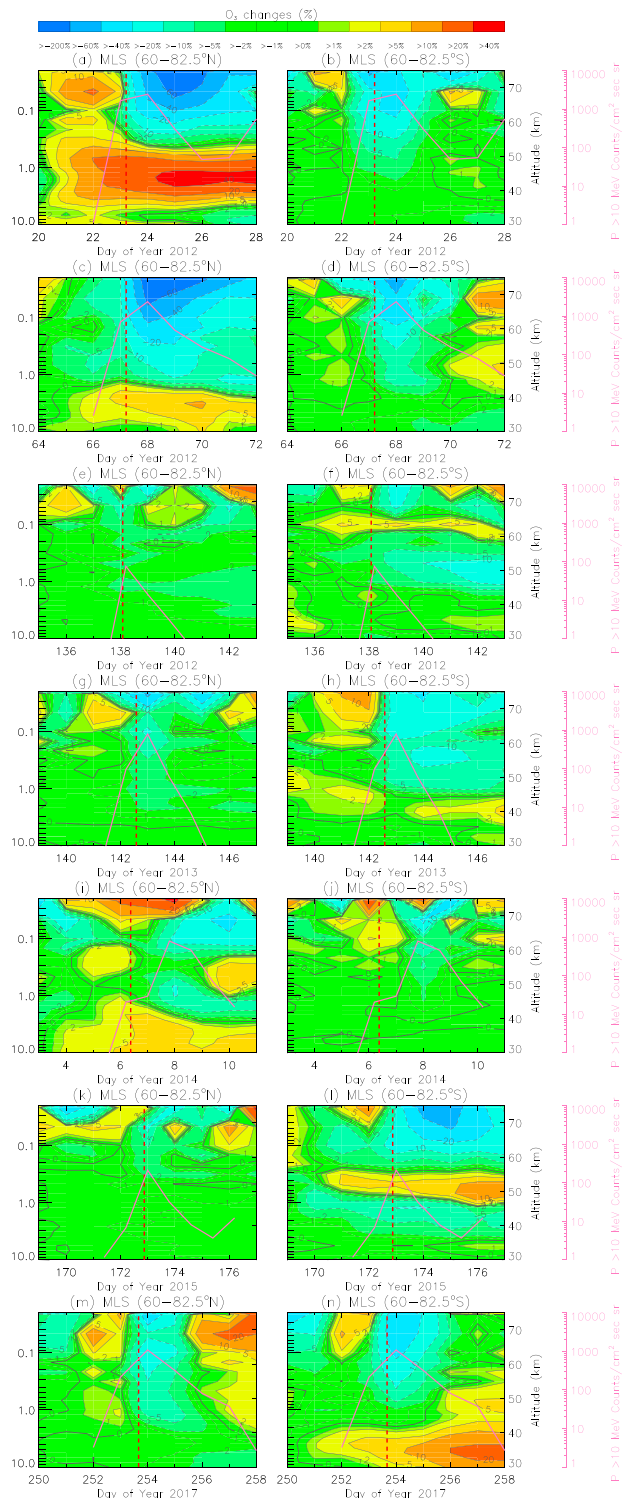


**Figure 3.** Daily averaged flux of proton with energies  $>10$  MeV from Geostationary Operational Environmental Satellites 13 and changes of ozone from Aura Microwave Limb Sounder for the (left)  $60\text{--}82.5^\circ\text{N}$  band and (right)  $60\text{--}82.5^\circ\text{S}$  band. Each numbered row corresponds to the numbered solar proton event (SPE) listed in Table 1. The contour intervals for the ozone changes are  $-60, -40, -20, -10, -5, -2, -1, 0, 1, 2, 5, 10, 20$ , and  $40\%$  of the background. The pink lines are the daily averaged proton flux during the SPEs. The dotted red lines indicate the start time of the SPEs.

ozone increase in the mesosphere above 1 hPa can also be related to the corresponding  $\text{HO}_2$  decrease. The similarity at about 0.1 hPa is particularly noticeable. The more than 10% increase of ozone near 0.04–0.07 hPa in 11 March 2012 in the northern hemisphere corresponds to the  $\text{HO}_2$  decrease in 10 March 2012 at the same level. The long-lasting increment to ozone of 5% at the pressure of 0.1 hPa in the southern hemisphere during the third SPE also corresponds to the  $\text{HO}_2$  decrease at the level of 0.2 hPa. The correlation between  $\text{HO}_2$  and ozone is discussed in the next section.

However, some abnormal MLS increases in ozone appeared. The ozone increases in 20–28 January 2012 greater than 0.5 hPa were due to the sudden stratospheric warming event which happened several days before the SPE (von Clarmann et al., 2013). The ozone increased dramatically then overwhelmed the effect of SPE.

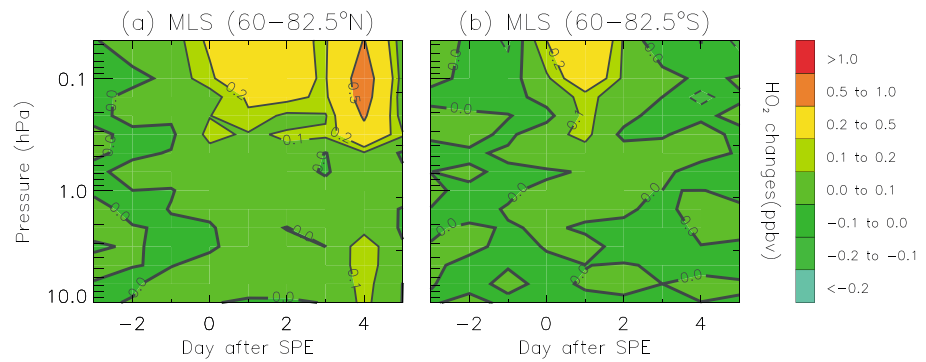
As expected, the ozone background concentration also has a season dependence, and it is opposite to  $\text{HO}_2$ . The background in the winter polar mesosphere is  $\sim 0.1\text{--}1$  ppmv greater than that in the summer polar mesosphere. This proved the fact that a higher  $\text{HO}_2$  concentration always corresponds to a lower ozone concentration. The  $\text{HO}_2$  increase, which occurred earlier, can contribute to ozone depletion during the SPE.

## 5. Composite Analysis

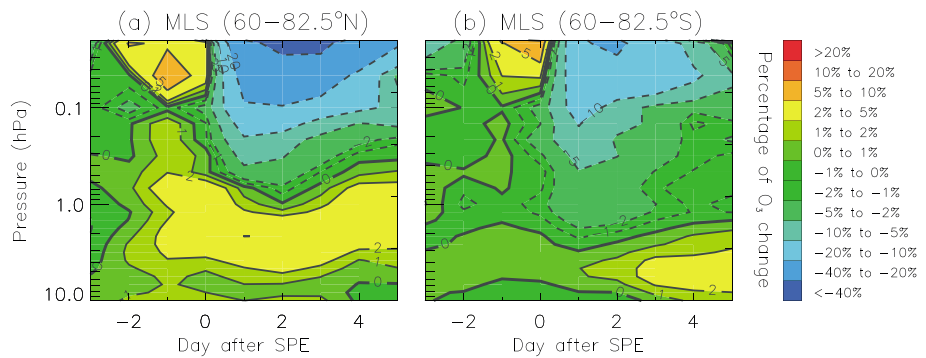
From the above sections, we conclude that the mesospheric constituents can be influenced by the energetic protons depositing energy into the atmosphere. In order to find the general temporal effects of SPE on compositions of the middle and upper atmosphere, we compose all the variations during the SPE together and then calculate the correlation coefficient between  $\text{HO}_2$  and ozone variations during the SPEs. Figure 4 shows the composite MLS observed  $\text{HO}_2$  changes during SPE. The  $\text{HO}_2$  enhancements start to appear the day the protons approach the Earth and last for 2 days in the southern hemisphere. The 4-day long lasting  $\text{HO}_2$  enhancements are due to the fifth substantial and late-occurred increase in the northern polar region in 10 January 2014. We composed six  $\text{HO}_2$  variations excluding the fifth one (not shown), then the  $\text{HO}_2$  variations in both of the hemispheres are very similar to Figure 4b. Thus, generally, the  $\text{HO}_2$  has a short-term response above 0.2 hPa to the big SPEs. The enhancement generally lasts 2 days.

Figure 5 shows the composite ozone changes during the SPE. The variations in the north and south polar regions are very similar in intensity and morphology. The maximum ozone decreases of  $>20\%$  occur approximately at 0.02 hPa the second day the SEP approaches the Earth. The ozone depletion comes out later than the  $\text{HO}_2$  increase. This phenomenon is observed in the single event, which further proves that the  $\text{HO}_2$  enhancement affects ozone depletion during the SPE. From Figure 5, we conclude that during a big SPE, ozone is reduced over a large altitude range less than 1.0 hPa in polar regions, and the depletion can last 7 days.

Figure 6 illustrates the spatial and temporal correlation between ozone and  $\text{HO}_2$  variations during the SPEs. In order to avoid the anomalous



**Figure 4.** Composite daily averaged  $\text{HO}_2$  changes from Aura Microwave Limb Sounder measurements during solar proton events in the (a) north polar regions and (b) south polar regions. The contour intervals for the  $\text{HO}_2$  changes are  $-0.5$ ,  $-0.2$ ,  $-0.1$ ,  $0.0$ ,  $0.1$ ,  $0.2$ ,  $0.5$ , and  $1.0$  ppbv.



**Figure 5.** Composite daily averaged ozone changes from Aura Microwave Limb Sounder measurements during solar proton events in the (a) north polar regions and (b) south polar regions. The contour intervals for the ozone changes are  $-40$ ,  $-20$ ,  $-10$ ,  $-5$ ,  $-2$ ,  $-1$ ,  $0$ ,  $1$ ,  $2$ ,  $5$ ,  $10$ , and  $20\%$  of the background.

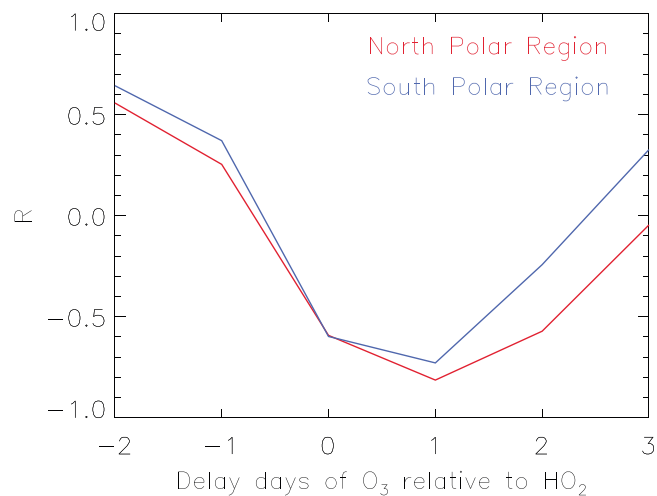


**Figure 6.** Correlation coefficient between relatively delayed change of ozone column density at a height of  $0.316\text{--}0.022$  hPa and change of  $\text{HO}_2$  column density at a height of  $0.316\text{--}0.046$  hPa during the solar proton events. The red fold line is the correlation coefficient of the ozone and  $\text{HO}_2$  over the north polar region, and the blue fold line is the correlation coefficient of the ozone and  $\text{HO}_2$  over the south polar region.

and extremely large enhancement in the northern hemisphere in the fifth SPE to bias the composite results, we remove the fifth event from the composition in the northern hemisphere. The column density of HO<sub>2</sub> changes significantly in the range of 0.215–0.046 hPa (Figure 4) and ozone changes in the range of 1.21–0.022 hPa (Figure 5). von Clarmann et al. (2013) showed that NO<sub>x</sub>-related ozone loss starts a couple of days after the SPE around 55 km (~0.4 hPa). To find the correlation between ozone and HO<sub>2</sub> changes, we narrow the ozone pressure range to 0.316–0.022 hPa, which is similar to the range of HO<sub>2</sub> changes and just above 0.4 hPa. The red fold line is the correlation coefficient of the ozone and HO<sub>2</sub> in the northern hemisphere, and the blue fold line is the correlation coefficient of the ozone and HO<sub>2</sub> in the southern hemisphere. Both of the strongest negative correlations of –0.81 and –0.73 in the northern and southern mesosphere occur at 1-day delay. This proves the existence of a negative correlation between the perturbations of HO<sub>2</sub> and ozone, and ozone is always affected by HO<sub>2</sub> during the SPEs.

## 6. Conclusions

Seven selected large SPEs from 2012 to 2017 within the solar cycle 24 showed significant influence on the middle and upper atmosphere over the polar regions. The MLS observed that HO<sub>2</sub> and ozone changed substantially. The HO<sub>2</sub> enhancement can be up to 1.0 ppbv during a strong SPE. The height of the HO<sub>2</sub> increase is above 0.2 hPa, and the peak always appears at 0.1 hPa. Generally, the HO<sub>2</sub> constitution increases larger than 0.2 ppbv and lasts 2 days. The maximum ozone depletion of 60% occurred in two SPEs in 2012. An averaged 10% reduction and duration of 7 days showed a large response of ozone to the SPEs. The ozone reduction at 0.02–1.0 hPa pressure altitude range shows that the ozone was affected by SPE more significantly.

The symmetrical changes of HO<sub>2</sub> and ozone during SPEs show a same response of the northern and southern mesospheric compositions to the large SPEs. Through the correlation analysis, the similarities in HO<sub>2</sub> and ozone perturbation and the later occurrence of ozone indicate that ozone is also affected by HO<sub>2</sub> variations in the mesosphere during SPEs.

## Acknowledgments

This work is supported by the National Natural Science Foundation of China (41774158, 41474129, 41674150, and 41704148), the Open Research Project of Large Research Infrastructures of CAS – “Study on the interaction between low/ mid-latitude atmosphere and ionosphere based on the Chinese Meridian Project”, and the Youth Innovation Promotion Association of the Chinese Academy of Sciences (2011324). We thank the NASA EOS Aura MLS team for providing free access to their data. We also acknowledge the use of the GOES Space Environment Monitor data provided by NOAA Space Weather Prediction Center over the Internet (<ftp://ftp.swpc.noaa.gov/pub/lists/particle/>). The ion pair production rates data sets are publicly provided by Charles Jackman (at the SOLARIS-HEPPA website <http://solarisheppa.geomar.de/solarprotonfluxes>). Aura/MLS data are available from <http://disc.sci.gsfc.nasa.gov/Aura/data-holdings/MLS>.

## References

- Andersson, M. E., Verronen, P. T., Rodger, C. J., Clilverd, M. A., & Wang, S. (2014). Longitudinal hotspots in the mesospheric OH variations due to energetic electron precipitation. *Atmospheric Chemistry and Physics*, 14(2), 1095–1105. <https://doi.org/10.5194/acp-14-1095-2014>
- Brown, R. (1968). Energetic electron precipitation in the auroral zone and its influence on atomic oxygen in the mesosphere. *Journal of Atmospheric and Terrestrial Physics*, 30(9), 1723–1728. [https://doi.org/10.1016/0021-9169\(68\)90022-6](https://doi.org/10.1016/0021-9169(68)90022-6)
- Crutzen, P. J., Isaksen, I. S., & Reid, G. C. (1975). Solar proton events: Stratospheric sources of nitric oxide. *Science*, 189(4201), 457–459. <https://doi.org/10.1126/science.189.4201.457>
- Damiani, A., Storini, M., Rafanelli, C., & Diego, P. (2010). The hydroxyl radical as an indicator of SEP fluxes in the high-latitude terrestrial atmosphere. *Advances in Space Research*, 46(9), 1225–1235. <https://doi.org/10.1016/j.asr.2010.06.022>
- Emslie, A. G., Dennis, B. R., Shih, A. Y., Chamberlin, P. C., Mewaldt, R. A., Moore, C. S., et al. (2012). Global energetics of thirty-eight large solar eruptive events. *The Astrophysical Journal*, 759(1), 71. <https://doi.org/10.1088/0004-637X/759/1/71>
- Frederick, J. E. (1976). Solar corpuscular emission and neutral chemistry in the Earth's middle atmosphere. *Journal of Geophysical Research*, 81(19), 3179–3186. <https://doi.org/10.1029/JA081i019p03179>
- Funke, B., García-Comas, M., López-Puertas, M., Glatthor, N., Stiller, G. P., von Clarmann, T., et al. (2008). Enhancement of N<sub>2</sub>O during the October–November 2003 solar proton events. *Atmospheric Chemistry and Physics*, 8(14), 3805–3815. <https://doi.org/10.5194/acp-8-3805-2008>
- Gopalswamy, N., Xie, H., Akiyama, S., Mäkelä, P. A., & Yashiro, S. (2014). Major solar eruptions and high-energy particle events during solar cycle 24. *Earth, Planets and Space*, 66(1), 104. <https://doi.org/10.1186/1880-5981-66-104>
- Gopalswamy, N., Xie, H., Akiyama, S., Yashiro, S., Usoskin, I. G., & Davila, J. M. (2013). The first ground level enhancement event of solar cycle 24: Direct observation of shock formation and particle release heights. *The Astrophysical Journal*, 765(2), L30. <https://doi.org/10.1088/2041-8205/765/2/L30>
- Heath, D. F., Krueger, A. J., & Crutzen, P. J. (1977). Solar proton event: Influence on stratospheric ozone. *Science*, 197(4306), 886–889. <https://doi.org/10.1126/science.197.4306.886>
- Jackman, C. H., DeLand, M. T., Labow, G. J., Fleming, E. L., Weisenstein, D. K., Ko, M. K. W., et al. (2005a). The influence of the several very large solar proton events in years 2000–2003 on the neutral middle atmosphere. *Advances in Space Research*, 35(3), 445–450. <https://doi.org/10.1016/j.asr.2004.09.006>
- Jackman, C. H., DeLand, M. T., Labow, G. J., Fleming, E. L., Weisenstein, D. K., Ko, M. K. W., et al. (2005b). Neutral atmospheric influences of the solar proton events in October–November 2003. *Journal of Geophysical Research*, 110, A09S27. <https://doi.org/10.1029/2004JA010888>
- Jackman, C. H., Frederick, J. E., & Stolarski, R. S. (1980). Production of odd nitrogen in the stratosphere and mesosphere: An intercomparison of source strengths. *Journal of Geophysical Research*, 85(C12), 7495–7505. <https://doi.org/10.1029/JC085iC12p07495>
- Jackman, C. H., Marsh, D. R., Vitt, F. M., García, R. R., Randall, C. E., Fleming, E. L., & Frith, S. M. (2009). Long-term middle atmospheric influence of very large solar proton events. *Journal of Geophysical Research*, 114, D11304. <https://doi.org/10.1029/2008JD011415>
- Jackman, C. H., Marsh, D. R., Vitt, F. M., Roble, R. G., Randall, C. E., Bernath, P. F., et al. (2011). Northern hemisphere atmospheric influence of the solar proton events and ground level enhancement in January 2005. *Atmospheric Chemistry and Physics*, 11(13), 6153–6166. <https://doi.org/10.5194/acp-11-6153-2011>



- Jackman, C. H., Randall, C. E., Harvey, V. L., Wang, S., Fleming, E. L., López-Puertas, M., et al. (2014). Middle atmospheric changes caused by the January and March 2012 solar proton events. *Atmospheric Chemistry and Physics*, 14(2), 1025–1038. <https://doi.org/10.5194/acp-14-1025-2014>
- Krivolutsky, A. A., Klyuchnikova, A. V., Zakharov, G. R., Vyushkova, T. Y., & Kuminov, A. A. (2006). Dynamical response of the middle atmosphere to solar proton event of July 2000: Three-dimensional model simulations. *Advances in Space Research*, 37(8), 1602–1613. <https://doi.org/10.1016/j.asr.2005.05.115>
- Li, C., Firoz, K. A., Sun, L. P., & Miroshnichenko, L. I. (2013). Electron and proton acceleration during the first ground level enhancement event of solar cycle 24. *The Astrophysical Journal*, 770(1), 34. <https://doi.org/10.1088/0004-637x/770/1/34>
- Livesey, N. J., Read, W. G., Wagner, P. A., Froidevaux, L., Lambert, A., Manney, G. L., et al. (2018). Earth Observing System (EOS) Aura Microwave Limb Sounder (MLS) version 4.2x level 2 data quality and description document, JPL D-33509 Rev. D. Retrieved from [https://mls.jpl.nasa.gov/data/v4-2\\_data\\_quality\\_document.pdf](https://mls.jpl.nasa.gov/data/v4-2_data_quality_document.pdf)
- López-Puertas, M., Funke, B., Gil-López, S., Von Clarmann, T., Stiller, G., Höpfner, M., et al. (2005). Observation of NO<sub>x</sub> enhancement and ozone depletion in the Northern and Southern Hemispheres after the October–November 2003 solar proton events. *Journal of Geophysical Research*, 110, A09S43. <https://doi.org/10.1029/2005JA011050>
- McPeters, R. D., & Jackman, C. H. (1985). The response of ozone to solar proton events during solar cycle 21: The observations. *Journal of Geophysical Research*, 90(D5), 7945–7954. <https://doi.org/10.1029/JD090iD05p07945>
- Newell, H. E., & Naugle, J. E. (1960). Radiation environment in space. *Science*, 132(3438), 1465–1472. <https://doi.org/10.1126/science.132.3438.1465>
- Nicolet, M. (1975). Stratospheric ozone: An introduction to its study. *Reviews of Geophysics*, 13(5), 593–636. <https://doi.org/10.1029/RG013i005p00593>
- Seppälä, A., Verronen, P. T., Kyrölä, E., Hassinen, S., Backman, L., Hauchecorne, A., et al. (2004). Solar proton events of October–November 2003: Ozone depletion in the Northern Hemisphere polar winter as seen by GOMOS/Envisat. *Geophysical Research Letters*, 31, L19107. <https://doi.org/10.1029/2004GL021042>
- Shea, M. A., & Smart, D. F. (2012). Space weather and the ground-level solar proton events of the 23rd solar cycle. *Space Science Reviews*, 171(1–4), 161–188. <https://doi.org/10.1007/s11214-012-9923-z>
- Sinnhuber, M., Nieder, H., & Wieters, N. (2012). Energetic particle precipitation and the chemistry of the mesosphere/lower thermosphere. *Surveys in Geophysics*, 33(6), 1281–1334. <https://doi.org/10.1007/s10712-012-9201-3>
- Solomon, S., Reid, G. C., Rusch, D. W., & Thomas, R. J. (1983). Mesospheric ozone depletion during the solar proton event of July 13, 1982 part II. Comparison between theory and measurements. *Geophysical Research Letters*, 10(4), 257–260. <https://doi.org/10.1029/GL010i004p00257>
- Solomon, S., Rusch, D. W., Gérard, J.-C., Reid, G. C., & Crutzen, P. J. (1981). The effect of particle precipitation events on the neutral and ion chemistry of the middle atmosphere: II. Odd hydrogen. *Planetary and Space Science*, 29(8), 885–893. [https://doi.org/10.1016/0032-0633\(81\)90078-7](https://doi.org/10.1016/0032-0633(81)90078-7)
- Swider, W., & Keneshea, T. J. (1973). Decrease of ozone and atomic oxygen in the lower mesosphere during a PCA event. *Planetary and Space Science*, 21(11), 1969–1973. [https://doi.org/10.1016/0032-0633\(73\)90126-8](https://doi.org/10.1016/0032-0633(73)90126-8)
- Thakur, N., Gopalswamy, N., Xie, H., Mäkelä, P., Yashiro, S., Akiyama, S., & Davila, J. M. (2014). Ground level enhancement in the 2014 January 6 solar energetic particle event. *The Astrophysical Journal*, 790(1), L13. <https://doi.org/10.1088/2041-8205/790/1/L13>
- Verkhoglyadova, O. P., Wang, S., Mlynarczyk, M. G., Hunt, L. A., & Zank, G. P. (2015). Effects of two large solar energetic particle events on middle atmosphere nighttime odd hydrogen and ozone content: Aura/MLS and TIMED/SABER measurements. *Journal of Geophysical Research: Space Physics*, 120, 12–29. <https://doi.org/10.1002/2014JA020609>
- Verkhoglyadova, O. P., Wissing, J. M., Wang, S., Kallenrode, M. B., & Zank, G. P. (2016). Nighttime mesospheric hydroxyl enhancements during SEP events and accompanying geomagnetic storms: Ionization rate modeling and Aura satellite observations. *Journal of Geophysical Research: Space Physics*, 121, 6017–6030. <https://doi.org/10.1002/2015JA022217>
- Verronen, P. T., Rodger, C. J., Clilverd, M. A., & Wang, S. (2011). First evidence of mesospheric hydroxyl response to electron precipitation from the radiation belts. *Journal of Geophysical Research*, 116, D07307. <https://doi.org/10.1029/2010JD014965>
- Verronen, P. T., Seppälä, A., Kyrölä, E., Tamminen, J., Pickett, H. M., & Turunen, E. (2006). Production of odd hydrogen in the mesosphere during the January 2005 solar proton event. *Geophysical Research Letters*, 33, L24811. <https://doi.org/10.1029/2006GL028115>
- von Clarmann, T., Funke, B., López-Puertas, M., Kellmann, S., Linden, A., Stiller, G. P., et al. (2013). The solar proton events in 2012 as observed by MIPAS. *Geophysical Research Letters*, 40, 2339–2343. <https://doi.org/10.1002/grl.50119>
- von Clarmann, T., Glatthor, N., Höpfner, M., Kellmann, S., Ruhnke, R., Stiller, G. P., et al. (2005). Experimental evidence of perturbed odd hydrogen and chlorine chemistry after the October 2003 solar proton events. *Journal of Geophysical Research*, 110, A09S45. <https://doi.org/10.1029/2005JA011053>
- Zawedde, A. E., Nesse Tysøy, H., Hibbins, R., Espy, P. J., Ødegaard, L. K. G., Sandanger, M. I., & Stadsnes, J. (2016). The impact of energetic electron precipitation on mesospheric hydroxyl during a year of solar minimum. *Journal of Geophysical Research: Space Physics*, 121, 5914–5929. <https://doi.org/10.1002/2016JA022371>